Journal of Power Sources 195 (2010) 8110–8115

Contents lists available at ScienceDirect

Journal of Power Sources

journal homepage: www.elsevier.com/locate/jpowsour

Towards a compact SU-8 micro-direct methanol fuel cell

J.P. Esquivel[a], T. Senn[b], P. Hernández-Fernández[c], J. Santander[a], M. Lörgen[b], S. Rojas[d], B. Löchel[b], C. Cané[a], N. Sabaté[a,*]

[a] Instituto de Microelectrónica de Barcelona, IMB-CNM (CSIC), Campus UAB, 08193 Bellaterra, Barcelona, Spain
[b] Helmholtz-Zentrum Berlin für Materialien und Energie GmbH, Application Centre for Microengineering, Albert-Einstein-Str. 15, 12489 Berlin, Germany
[c] Dpto. Química-Física Aplicada, Facultad de Ciencias, Universidad Autónoma de Madrid (UAM), C/Francisco Tomás y Valiente 7, 28049 Madrid, Spain
[d] Instituto de Catálisis y Petroleoquímica (CSIC), C/Marie Curie 2, 28049 Madrid, Spain

ARTICLE INFO

Article history:
Received 4 June 2010
Received in revised form 5 July 2010
Accepted 17 July 2010
Available online 23 July 2010

Keywords:
SU-8
Photoresist
Micro-fuel cell
All-polymer
DMFC
PowerMEMS

ABSTRACT

This paper presents an all-polymer micro-direct methanol fuel cell (microDMFC) fabricated with SU-8 photoresist. The present development exploits the capability of SU-8 components to bond to each other by a hot-pressing process and obtain a compact device. The device is formed by a membrane electrode assembly (MEA) sandwiched between two current collectors. The MEA consists of a porous SU-8 membrane filled with a proton exchange polymer and covered by a thin layer of carbon-based electrodes with a low catalyst loading (1.0 mg cm^{-2}). The current collectors consist of two metalized SU-8 plates provided with a grid of through-holes that allow delivering the reactants to the MEA by diffusion. Fuel cell characterization was performed by measuring the polarization curves under different methanol concentrations and temperatures. The components were first tested using an external casing. A maximum power density of 4.15 mW cm^{-2} was measured with this assembly working with a 4 M methanol concentration and at a temperature of 40 °C. The components were then bonded to obtain a compact micro-direct methanol fuel cell that yielded a power density of 0.65 mW cm^{-2} under the same conditions. Despite this decrease in power density after bonding, the drastic reduction of the device dimensions resulted in an increase of more than 50 times the previous volumetric power density. The results obtained validate this novel approach to an all-polymer micro-fuel cell.

1. Introduction

The demand for miniaturized power sources has increased rapidly in the past few years due to the spread of portable electronic applications. Many different approaches have been developed to address this need using micromachining technologies. In this respect, micro-fuel cells have gained interest as portable power sources due to their high theoretical efficiency and energy density. Fuel cells promise to provide more reliable, longer portable power than batteries as their energy is stored as a fuel instead of being a part of the power source [1–3]. Miniaturization of these power generating devices promises higher efficiency and performance but the complete system integration remains a key challenge. In most reported cases, micro-fuel cell architectures require complex and bulky packaging to hold the components together. Nevertheless, innovative micro-fuel cell designs have been proposed as alternatives to achieve highly compact systems [4–6].

In the search for a completely integrated and low cost device, polymeric materials have recently been proposed to produce micro-fuel cell components. Due to their fast and versatile microfabrication methods, polymers have already proven to be suitable for an assortment of on-chip functions and applications [7]. Interesting approaches have been reported in the last few years concerning micro-fuel cell developments, e.g. Shah et al. [8] used different microfabrication techniques to develop a micro-fuel cell where polydimethylsiloxane (PDMS) was used as cell support and housing and Chan et al. [9] micromachined Gaussian-shaped microchannels in polymethylmethacrylate (PMMA) using a CO_2-laser obtaining a high power hydrogen-fed micro-fuel cell. Moreover, UV-sensitive resists such as SU-8 have proved to be excellent candidates to obtain small and very precise microstructured polymeric components [10], e.g. Hsieh et al. [11] reported the use of metalized UV-sensitive resist to obtain flow field plates and Cha et al. [12] used the same material to fabricate current collectors in one of the first reported attempts of obtaining an all-polymer microDMFC. Recently, Weinmueller et al. [13] reported a micro-direct methanol fuel cell based on the microstructuring of a

* Corresponding author at: Instituto de Microelectrónica de Barcelona, IMB-CNM (CSIC), Micro and Nanosystems Department, Campus UAB sn, 08193 Bellaterra, Barcelona, Spain. Tel.: +34 93 594 77 00; fax: +34 93 580 14 96.
E-mail address: neus.sabate@imb-cnm.csic.es (N. Sabaté).

0378-7753/$ – see front matter © 2010 Elsevier B.V. All rights reserved.
doi:10.1016/j.jpowsour.2010.07.050

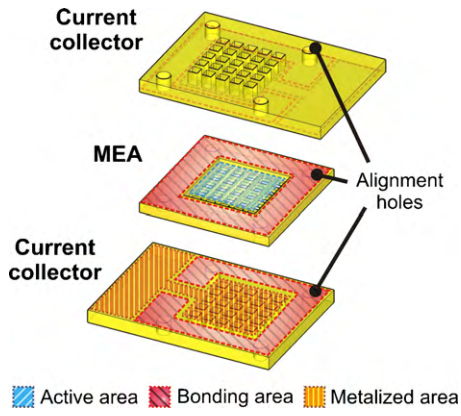

Fig. 1. Exploded view of SU-8 micro-fuel cell components with main parts identified.

metalized thin photosensitive polymer film, in which the flexible capabilities of SU-8 resist were emphasized.

In this paper, we present a compact microDMFC where all components are fabricated with SU-8 resists. Furthermore, the present development takes advantage not only of the above-mentioned structural and mechanical properties of these resists but also exploits the capability of SU-8 components to bond to each other by a hot-pressing process to obtain a compact micro-direct methanol fuel cell. In addition, issues such as the reduction of device complexity and final cost have determined the device design, conceived to work under passive operation (fuel transport by diffusion) with a minimum amount of Pt catalyst. As will be shown, all fuel cell components are first independently characterized and validated. Then, assembly is carried out to evaluate the fuel cell performance under different methanol concentrations and temperatures.

2. Description of device design

The aim of the present development was obtaining a simple and compact design of a micro-fuel cell. For this reason, the system is based on a diffusion-driven feeding of methanol and air, which reduces complexity and allows elimination of all ancillary devices. The proposed micro-fuel cell consists of an assembly of three components made of SU-8 photoresist: a membrane electrode assembly (MEA) sandwiched between two current collectors. Fig. 1 depicts an exploded view of the proposed fuel cell showing the basic structure of both MEA and current collectors.

The MEA consists of a 10 mm × 10 mm wide SU-8 membrane with a central area of 5 mm × 5 mm provided with an ordered array of square micropores. These micropores are filled with a proton exchange polymer and are responsible of the proton conductivity of the SU-8 membrane. In this configuration, the SU-8 structure acts as a mechanical support of the proton-conducting polymer and at the same time offers the possibility of being bonded directly to other SU-8 fuel cell components. Total thickness of the SU-8 membrane was set at 170 μm, as this is the nominal thickness of a Nafion® 117 film, which is the polymeric electrolyte membrane typically used in direct methanol fuel cells. Membranes with three different array designs were fabricated; the micropores side-length was fixed at 250 μm and increasing membrane open ratios were defined by setting pore separations at 250, 100 and 50 μm in order to maximize proton-conductive area without compromising the mechanical stability of the SU-8 structure. After that, the active area was coated with thin layers of carbon-based electrodes. The SU-8 frame around the active area was left uncovered for subsequent bonding to the current collectors.

The SU-8 current collectors have a dimension of 10 mm × 14 mm and a thickness of 250 μm. The structures are also provided with a grid of through-holes over a 5 mm × 5 mm area that is coincident with the active area of the MEA. In this way, the SU-8 structures act as current collectors, and at the same time deliver the reactants to both sides of the MEA by diffusion. In this case, two different designs of current collector were fabricated for anode and cathode sides; both designs are provided with squared through-holes of 100 μm side-length but separations between holes are set at 50 μm at the anode and 100 μm at the cathode. It has been demonstrated that in passive microDMFC the unbalancing of cathode and anode open ratios (e.g. area exposed to reactants versus total area) prevents cathode flooding and minimizes methanol crossover [14]. Electrical conductivity of the structures was provided by partially metalizing their surface. A surrounding frame was left uncovered to allow bonding to the MEA, as is indicated in Fig. 1.

3. Fabrication and characterization of SU-8 fuel cell components

The photolithography process was optimized for obtaining suitable released SU-8 structures that were able to bond to each other by a subsequent hot-pressing process. Lithography parameters such as baking times and exposure dose have to be adjusted to find a trade-off between a full exposure and a photoresist polymerization level suitable for thermal bonding [15].

The lithography of the SU-8 components was performed on 500 μm thick, single side polished, 100 mm Si wafers. The first step consisted of the deposition of a sacrificial layer that will be removed at the end of the process to release the SU-8 structures. For this, a layer of Omnicoat™ (Microchem Corp., Newton, MA, USA) was spin-coated onto the substrate (speed: 2000 rpm, time: 35 s) followed by a baking step of 1 min at 200 °C to vaporize the solvent. From this point different processes were used for the fabrication of the current collectors and the membrane electrode assemblies. Current collectors were fabricated using a single layer of SU-8 100, while membranes needed a multilayer process of SU-8 50 (both from Microchem Corp.).

3.1. Fabrication of the membrane electrode assembly

The fabrication of the SU-8 membrane electrode assembly consists of a series of steps that can be grouped in three main stages: (1) obtaining of the photoresist structures by the UV lithography process; (2) functionalization of the membranes by filling the cavities in the membranes with a proton exchange polymer and (3) carbon-based electrode deposition by air spray. Each of these steps is described in detail in the following sections and can be followed in Fig. 2.

3.1.1. SU-8 porous structure

The SU-8 membrane is composed by two SU-8 layers. The first layer defines an ordered array of square micropores over an area of 5 mm × 5 mm centered in the membrane. The second layer defines a 2.5 mm wide frame around the micropore array. For its fabrication, the first layer of SU-8 50 was spin-coated at 2000 rpm for 35 s to give a thickness of 50 μm. The soft-bake of this layer consisted of a 60 min at 25 °C, 6 min at 65 °C, 30 min at 95 °C and 10 h cool-down to 25 °C on a hot-plate using linear ramps between temperatures. The UV-exposure was performed with a MA6/BA6 mask aligner (Karl Süss MicroTec GmbH, Garching, Germany) with a dose of 190 mJ cm^{-2} using a printed transparent foil as mask that defined the membrane with the array of micropores. Post-exposure bake consisted of 1 min at 65 °C on a hot-plate followed by 5 min at 95 °C in a convection oven. Then the second SU-8 50 layer was

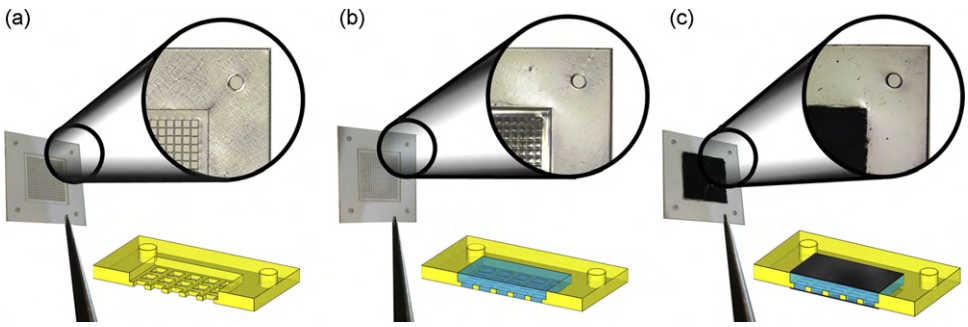

Fig. 2. Pictures and cross-sectional views of the different stages in the Membrane Electrode Assembly fabrication: (a) SU-8 porous membrane released from substrate, (b) filling of micropores with Nafion® and (c) carbon-based electrodes deposition. The magnifications show a circular area of 5 mm diameter.

spin-coated at 1000 rpm for 35 s to obtain a layer of 120 μm thickness. The soft-bake of this second layer consisted of 60 min at 25 °C, 6 min at 65 °C, 60 min at 75 °C and 10 h cool-down to 25 °C on a hot-plate. The exposure of this layer was performed with a dose of 270 mJ cm^{-2} using a mask that defined the frame around the array of micropores in the membrane. Post-exposure bake consisted of 1 min at 65 °C in a hot-plate followed by 12 min at 95 °C in a convection oven. Finally, both layers were simultaneously developed in mr-600 Dev (Micro Resist Technologies GmbH, Berlin, Germany) for 30 min with agitation, then rinsed in 2-propanol and deionized water. To release the developed SU-8 structures from the substrate, the Omnicoat™ layer was removed by soaking the wafers in developer ma-D 332/S (Micro Resist Technologies GmbH) with agitation. The duration of this step varied from few minutes to several hours depending on the geometrical design of SU-8 structure. Fig. 2a shows a picture and cross-sectional view of the fabricated SU-8 porous membrane.

3.1.2. *Nafion®-filled SU-8 membranes*

In order to provide the SU-8 membranes with the required proton conductivity, their microperforations were filled with a liquid solution of proton exchange polymer (in this case, Nafion® perfluorinated resin solution 20 wt.% in lower aliphatic alcohols and water from Sigma–Aldrich, St. Louis, USA) that solidified after solvent evaporation. The empty cavities of both SU-8 layers (50 μm-thick grid and 120 μm-thick frame) were filled using a micropipette with solution volumes of 20–25 μl depending on the membrane design. The squared frame defined by the second lithography level served as a reservoir of Nafion® solution during filling and the subsequent solvent evaporation. In this way the Nafion® could be limited to the desired area, avoiding any dripping or spoiling, and the content in each membrane was accurately controlled. Fig. 2b shows a picture and cross-sectional view of the Nafion®-filled SU-8 porous membrane.

The proton-conductive capabilities of the Nafion®-filled SU-8 membranes were evaluated by electrochemical impedance spectroscopy (EIS). As the Nafion® resin solution used to fill the membranes was supplied in H^+ form, it was not necessary to activate the membranes prior to the measurement. Therefore the membranes were only hydrated soaking them in deionized water at 80 °C for 3 h inside a custom made support that prevented the SU-8 structure of being deformed by the temperature. The setup used to obtain the measurements consisted of a symmetrical electrochemical cell where the membranes were placed between two Pt thin plates. EIS measurements were performed using an Impedance/Gain-Phase Analyzer (SI 1260, Solartron Analytical, Farnborough, UK) in the frequency range from 0.1 Hz to 1 MHz and small ac voltage amplitude in the range between 25 and 100 mV at room temperature in water saturated ambient air (R.H. = 100%). Impedance spectra were acquired and analyzed with ZPlot and ZView software (Scribner Associates Inc., Southern Pines, USA). Before measuring the membrane conductivity, the electrodes of the cell were short-circuited in order to determine the contact resistance. This series resistance was considered as an offset for the cell measurements. Fig. 3 shows the Nyquist plot of the EIS measurements obtained from the different types of membrane. The insert shows a detail of the high-frequency range of impedance. Proton-conductivity values of the membranes were calculated following the analysis procedure described elsewhere [16]. Table 1 shows a summary of the main characteristics of the membranes and the calculated proton-conductivity values.

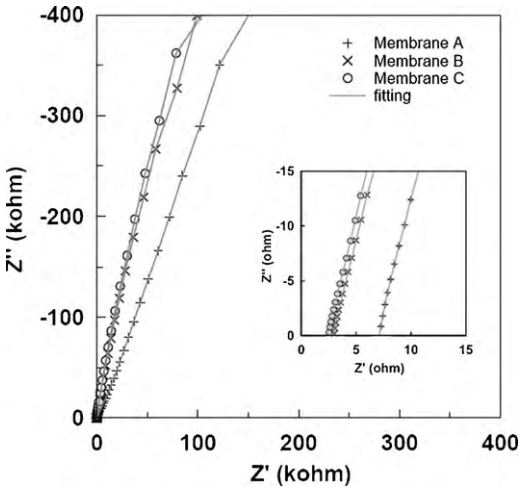

Fig. 3. Nyquist plot of the EIS measurements for the different Nafion®-filled SU-8 membranes at room temperature in air. The insert shows details of high-frequency impedance values.

It can be seen that the obtained proton conductivity of the hybrid membranes (σ_{total}) was 10 ± 1, 23 ± 1 and 28 ± 1 mS cm^{-1} for membranes A, B and C respectively. These values were obtained by

Table 1
Summary of membrane parameters and measured proton conductivities.

	Pore size-separation (μm)	A_{active} (cm^2)	A_{active}/A_{total}	σ_{active} (10^{-3} S cm^{-1})	σ_{total} (10^{-3} S cm^{-1})
Membrane A	250–250	0.0625	0.25	40 ± 2	10 ± 1
Membrane B	250–100	0.1225	0.49	46 ± 2	23 ± 1
Membrane C	250–50	0.1600	0.64	43 ± 2	28 ± 1

considering an effective membrane area of 5 mm × 5 mm (A_{total}), that is, including the contribution of the non-active SU-8 part of the membrane. Taking into account only the area filled by Nafion® polymer, the values of conductivity associated with the electrolyte (σ_{active}) resulted to be very similar between all membranes, with values around 43 ± 2 mS cm^{-1}, which is in accordance to the values reported in the literature for continuous Nafion® films [17]. These results confirmed the correct operation of the proton-conductive polymer once embedded in the SU-8 porous matrix. The variability found in the value of conductivity for the different supporting matrices could be attributed to slight discrepancies in the real membrane thickness from the 170 μm value used for calculations.

After measurements, all the fabricated membranes showed good mechanical stability. No fracture or significant buckling were observed, which proved that the SU-8 matrix was capable of holding the volume expansion of hydrated Nafion® without affecting its structure. For that reason, SU-8 membranes with the highest open ratio were used to fabricate the MEAs for the micro-fuel cell.

3.1.3. Carbon-based electrode layers

The deposition of the catalyst was performed by spraying a catalyst ink over the selected membranes. In order to define the active area where the catalyst are deposited, the membranes where placed between plastic foils from which 5 mm × 5 mm squares were cut out. In this way, the foils acted as a stencil during catalyst spraying. The preparation of the catalyst suspension was made by mixing the catalyst (30 wt.% as Pt on Cabot Vulcan XC72, atomic ratio Pt:Ru 1:1 for the anode and Pt/C 40 wt.% for the cathode, Johnson Matthey, London, UK), Nafion® ionomer 5 wt.% solution (Aldrich), isopropanol (Merck, Darmstadt, Germany) and Mili-Q water. Nafion® content in the ink was 55 wt.%. The amount of Nafion® in the ink has been optimized to avoid the flooding of the electrodes or the decrease in the performance of the single cell [18,19]. The suspension was dispersed in an ultrasonic bath for 45 min. Then, the ink was sprayed on one side of the membrane and the overall process was repeated to deposit the catalyst on the other side of the membrane. In either case, metal loading was 1.0 mg cm^{-2} (being the Pt loading 0.7 mg cm^{-2} at the anode and 1 mg cm^{-2} at the cathode). Fig. 2c shows a picture and cross-sectional view of the SU-8 MEA thus obtained.

3.2. Fabrication of fuel cell current collectors

For the fabrication of the SU-8 current collectors a layer of SU-8 100 was spin-coated over the wafer at 1000 rpm for 35 s to obtain a 250 μm thick layer. The soft-bake consisted of a series of temperature steps performed over a hot plate starting with a 60 min resting period at 25 °C, followed by 6 min at 65 °C, 90 min at 95 °C and 10 h cool-down to 25 °C. The UV-exposure was performed with a dose of 400 mJ cm^{-2}. Post-exposure bake consisted of 1 min at 65 °C in a hot-plate followed by 20 min at 95 °C in a convection oven. Finally, the layer was developed with agitation for 1 h in mr-600 Dev and then rinsed in 2-propanol and deionized water. The developed SU-8 collectors were released from the substrate removing the Omnicoat™ layer in developer ma-D 332/S with agitation.

In order to provide SU-8 current collectors with electrical conductivity, a bi-layer of 50 nm Ti and 50 nm Ni was deposited on one of their sides by sputtering (MRC-903, MRC Systems, Heidelberg, Germany). A tailored piece of polydimethylsiloxane (PDMS) was placed as a shadow mask onto the current collector to restrain metal deposition to the central 5 mm × 5 mm active area. In this way, the surrounding surface of the active area keeps SU-8 exposed and available to bond directly to the SU-8 MEA by hot-pressing. After this, the PDMS mask was peeled off from the SU-8 structure, leaving the metal layer on the desired places. The sputtered layer was then used as a seed layer for an electrodeposition of 1.5 μm of Ni and a thin layer of Au to prevent oxidation.

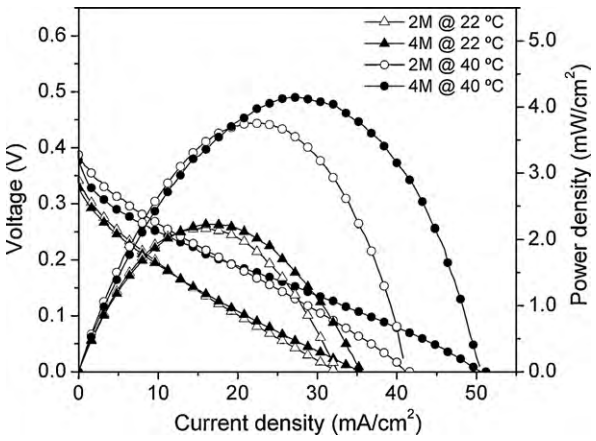

Fig. 4. Polarization curves of SU-8 micro-fuel cell with an external casing or frame operating on 2 and 4 M methanol concentrations at two temperatures.

The electrical resistivity of the SU-8 current collectors was characterized by 4-probe measurements performed on a test sample with the same metallization but with appropriate dimensions. The sheet resistance of the metal yielded a value of 46.6 mΩ per square, which was in accordance to the materials nominal resistance for the thickness deposited.

4. Results and discussion

4.1. Micro-fuel cell assembly and characterization

Once all the components were obtained separately, the micro-fuel cell was mounted by aligning two current collectors at both sides of the MEA. Before proceeding to the thermal bonding of all these SU-8 components, a preliminary test of the SU-8 fuel cell was performed using the same external casing that was developed for an analogous silicon micro-fuel cell approach [14]. The components were encapsulated by placing them between two machined methacrylate pieces that were tightened by 4 screws. A square window of 5.2 mm × 5.2 mm was milled through the acrylic pieces to allow the access of reactants (diluted methanol and air) towards the active areas through the current collectors. A rounded rabbet on one edge of both pieces was defined to fit the electrical connectors to the current collectors.

The polarization curve of the micro-fuel cell was obtained galvanostatically with a Keithley 2400 Sourcemeter (Keithley, Cleveland, USA) using an in-house LabVIEW (National Instruments, Austin, USA) program. Characterization was done with methanol concentrations of 2 M and 4 M (chosen because these values lie within the concentration range that yields optimal fuel cell performance in passive devices [20]), and at temperatures of 22 °C (room temperature) and 40 °C. Fig. 4 shows the polarization curves obtained with this assembly.

It can be seen that at room temperature (22 °C), the micro-fuel cell achieves a maximum power density of 2.20 mW cm^{-2} regardless of the methanol concentration. No significant differences in the open circuit voltage (OCV) are observed due to methanol crossover and the *I–V* curves are mainly controlled by ohmic losses. When increasing cell temperature to 40 °C, maximum power densities rise to 3.75 mW cm^{-2} and 4.15 mW cm^{-2} at fuel concentrations of 2 and 4 M, respectively. This is mainly due to the improvement of micro-fuel cell performance in the ohmic region due to the enhancement in the Nafion® proton conductivity at increasing temperatures. This time, a visible improvement in the transport-limited region of the

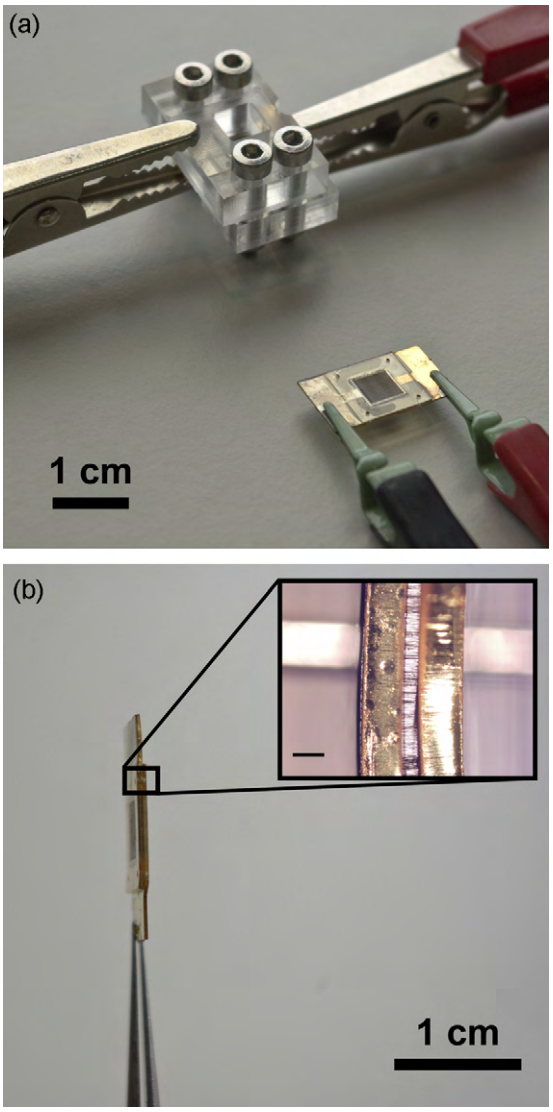

Fig. 5. (a) Picture of the two micro-fuel cell assemblies during characterization. (b) Side view of the SU-8 micro-fuel cell (the scale bar in the inset corresponds to 200 μm).

I–V curve can be observed when raising the methanol concentration from 2 to 4 M.

After this test, the SU-8 structures were bonded against each other by a hot-pressing process to obtain the compact device. A dedicated support was fabricated to align and press together the current collectors and the MEA. Alignment was done by inserting four needles through the small circular holes placed at the corners of SU-8 components. The assembly was then placed in a commercial hot-press (P/O/Weber, Remshalden, Germany) and heated to 85 °C for 10 min and 120 °C with a force of 2 kN for 20 min. After this, the assembly was cooled down by natural convection and the bonded SU-8 micro-fuel cell was released for testing. With this assembly, the total volume of the device is reduced more than 50 times (0.12 cm^3 respect to 6.75 cm^3). Fig. 5a and b shows photographs of the two assemblies tested, and a side view of the compact device where the significant size reduction between both approaches is clearly seen.

Characterization was done under the same conditions as with the previous setup. Fig. 6 shows the polarization curves obtained. After bonding, all curves present higher voltage values at open circuit conditions (500–580 mV) followed by a sudden voltage drop due to activation losses. After that, curves are mainly controlled by

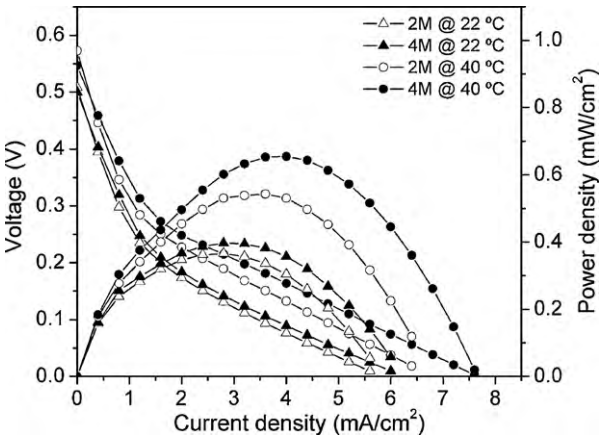

Fig. 6. Polarization curves of the compact SU-8 micro-fuel cell operating on 2 and 4 M methanol concentrations at two temperatures.

ohmic losses, showing no limitations in the mass transport region. In this case, the micro-fuel cell yielded a very similar maximum power density at both tested methanol concentrations and working temperatures. At 2 M concentration, a temperature increase from 22 to 40 °C raised the power density from 0.35 to 0.55 mW cm^{-2}, whereas at 4 M raised it from 0.40 to 0.65 mW cm^{-2}.

4.2. Discussion

Results show a clear difference in the power delivered by the SU-8 micro-fuel cell depending on the assembly setup. When tightened with an external acrylic casing, the maximum power of 4.15 mW cm^{-2} obtained at 40 °C and 4 M methanol concentration is comparable to results reported in the literature for other microDMFC partially fabricated with SU-8 components [12,13]. It is important to notice that unlike those used in previous works, the present approach reduces both device complexity and cost by using a diffusion-driven feeding of methanol and air and minimizing the amount of Pt catalyst to 1 mg cm^{-2}. Moreover, the continuous Nafion® film typically used in other approaches has been substituted here by a Nafion®-filled porous SU-8 membrane. The use of the membrane clearly enhances the level of integration of the final device, although it reduces the available proton-conductive area by a 36%.

When bonded together in a compact device, the maximum power density yielded by the SU-8 fuel cell decreases to 0.65 mW cm^{-2}. This is due to an increase of voltage losses in the ohmic region of the polarization curves. It can be seen that curves from Fig. 6 present the same slope regardless of temperature and methanol concentration, which indicates the existence of a significant contact resistance between the membrane and the current collectors. That is, even though the SU-8 components have been satisfactorily bonded and no fuel leakage has been observed, the pressure applied between them is lower than the one exerted by the external casing. Nevertheless, despite the decrease in its performance, the drastic reduction of the device dimensions achieved with this approach results in a substantial enhancement of volumetric power density from 0.15 mW cm^{-3} using the external casing up to 1.35 mW cm^{-3} in the compact approach.

5. Conclusions

In this work a novel approach to an all-polymer micro-fuel cell based on SU-8 photoresist has been presented. All fuel cell components (current collectors and MEA) are fabricated with the same material, whose bonding capabilities are exploited to obtain

a highly compact device. The integration is achieved in two steps; first, by the embedding of a polymeric electrolyte into a porous SU-8 membrane and second by bonding all SU-8 components together.

The micro-fuel cell has been first characterized using an external casing or frame to validate the functionality of its components. Despite the simplicity associated to the passive delivery of the fuel and the low catalyst content, the performance of the present micro-fuel cell is comparable to the few polymeric devices reported to date. After validation, all components were bonded together by hot-pressing in order to obtain the compact device. Characterization of the assembly showed a decrease in power density due to an increase in contact resistance. However, the drastic reduction of the device dimensions when dispensing with the external frame resulted in a larger volumetric power density.

Further work will be directed to device optimization through the reduction of ohmic losses. In this sense, different strategies arise, such as modification of the SU-8 structures that allow an increase of device robustness after thermal bonding; alternative MEA fabrication by substituting the carbon-based electrodes by a thinner catalyst layers (sputtering, electrodeposition, carbon nanotube incorporation); and the development of planar architectures in which pressure between components is not a key factor.

Nevertheless, the results presented demonstrate the potential of this approach to obtain a fully polymeric power source. They benefit from the advantages associated to SU-8 technology (e.g. high chemical and mechanical stability of structures, high resolution of patterns, low cost). Moreover, the use of this technology offers additional opportunities for integration of micro-fuel cell within a wide variety of polymeric devices such as lab-on-chip and other microfluidic platforms.

Acknowledgements

This work was partially supported by the Spanish Government project MICAELA-TEC2009-14660-C02-01. J.P. Esquivel and N. Sabaté would like to thank the financial support received from their respective doctoral and postdoctoral programs JAE-Predoc (CSIC) and Ramon y Cajal (MEC).

References

[1] N. Nam-Trung, C. Siew Hwa, Journal of Micromechanics and Microengineering 16 (4) (2006) R1.
[2] A. Kundu, J.H. Jang, J.H. Gil, C.R. Jung, H.R. Lee, S.H. Kim, B. Ku, Y.S. Oh, Journal of Power Sources 170 (1) (2007) 67–78.
[3] S.K. Kamarudin, W.R.W. Daud, S.L. Ho, U.A. Hasran, Journal of Power Sources 163 (2) (2007) 743–754.
[4] R. Hahn, S. Wagner, A. Schmitz, H. Reichl, Journal of Power Sources 131 (1–2) (2004) 73–78.
[5] T. Ito, M. Kunimatsu, Electrochemistry Communications 8 (1) (2006) 91–94.
[6] N. Kuriyama, T. Kubota, D. Okamura, T. Suzuki, J. Sasahara, Sensors and Actuators A: Physical 145–146 (2008) 354–362.
[7] G.S. Fiorini, D.T. Chiu, BioTechniques 38 (3) (2005) 18.
[8] K. Shah, W.C. Shin, R.S. Besser, Sensors and Actuators B: Chemical 97 (2–3) (2004) 157–167.
[9] S.H. Chan, N.T. Nguyen, Z.T. Xia, Z.G. Wu, Journal of Micromechanics and Microengineering 15 (1) (2005) 231–236.
[10] A.d. Campo, C. Greiner, Journal of Micromechanics and Microengineering 17 (6) (2007) R81.
[11] S.S. Hsieh, J.K. Kuo, C.F. Hwang, H.H. Tsai, Microsystem Technologies 10 (2) (2004) 121–126.
[12] H.-Y. Cha, H.-G. Choi, J.-D. Nam, Y. Lee, S.M. Cho, E.-S. Lee, J.-K. Lee, C.-H. Chung, Electrochimica Acta 50 (2–3) (2004) 795–799.
[13] C. Weinmueller, G. Tautschnig, N. Hotz, D. Poulikakos, Journal of Power Sources 195 (12) (2010) 3849–3857.
[14] J.P. Esquivel, N. Sabaté, J. Santander, N. Torres-Herrero, I. Gràcia, P. Ivanov, L. Fonseca, C. Cané, Journal of Power Sources 194 (1) (2009) 391–396.
[15] F.J. Blanco, M. Agirregabiria, J. Garcia, J. Berganzo, M. Tijero, M.T. Arroyo, J.M. Ruano, I. Aramburu, K. Mayora, Journal of Micromechanics and Microengineering 14 (7) (2004) 1047.
[16] J.P. Esquivel, N. Sabaté, A. Tarancón, N. Torres-Herrero, D. Dávila, J. Santander, I. Gràcia, C. Cané, Journal of Micromechanics and Microengineering 19 (6) (2009) 065006.
[17] V. Neburchilov, J. Martin, H. Wang, J. Zhang, Journal of Power Sources 169 (2) (2007) 221–238.
[18] J. Ihonen, F. Jaouen, G. Lindbergh, A. Lundblad, G. Sundholm, Journal of the Electrochemical Society 149 (2002) A448.
[19] G. Sasikumar, J.W. Ihm, H. Ryu, Electrochimica Acta 50 (2004) 601.
[20] J. Esquivel, N. Sabaté, J. Santander, N. Torres, C. Cané, Microsystem Technologies 14 (4) (2008) 535–541.